HHS Public Access

Author manuscript

Pediatr Radiol. Author manuscript; available in PMC 2021 December 01.

Published in final edited form as:

Pediatr Radiol. 2021 December ; 51(13): 2521–2529. doi:10.1007/s00247-021-05156-y.

Ferumoxytol-MRI Detects Joint and Pleural Infiltration of Bone Sarcomas in Pediatric and Young Adult Patients

Ashok J. Theruvath[1], **Ali Rashidi**[1], **Ramya Nyalakonda**[1], **Raffi Avedian**[3], **Robert Steffner**[3], **Sheri L. Spunt**[2], **Heike E. Daldrup-Link**[1,2]

[1]Department of Radiology, Pediatric Molecular Imaging Program, Stanford University

[2]Department of Pediatrics, Pediatric Hematology/Oncology, Lucile Packard Children's Hospital,

[3]Department of Orthopedic Surgery, Lucile Packard Children's Hospital, Stanford University

Abstract

Background: The diagnosis of joint infiltration by a malignant bone tumor affects surgical management. The specificity of standard MRI for diagnosing joint infiltration is limited. During our MRI evaluations with ferumoxytol nanoparticles of pediatric and young adult patients with bone sarcomas, we observed a surprising marked T1-enhancement of joint and pleural effusions in some patients and not others.

Objective: To evaluate, if nanoparticle extravasation differed between joints and pleura with and without tumor infiltration.

Materials and methods: We retrospectively identified 15 pediatric and young adult patients (mean age 16±4 years) with bone sarcomas who underwent 18 MRI scans at 1 hour (n=7) or 24 hours (n=11) after intravenous ferumoxytol infusion. Twelve patients also received a gadolinium(Gd)-enhanced MRI. We determined the presence or absence of tumor invasion into the joint or pleural space, based on histology (n=11) and imaging findings (n=4). We compared the signal-to-noise ratio (SNR) and contrast-to-noise ratio (CNR) of the joint or pleural fluid for tumors with and without invasion using a Mann-Whitney test.

Corresponding author: Heike E. Daldrup-Link MD PhD, Professor of Radiology and by courtesy of Pediatrics, Department of Radiology, Molecular Imaging Program at Stanford, Stanford University, 725 Welch Road, Stanford, CA 94304, USA; heiked@stanford.edu; phone: (650) 497-8601.

Author's contributions

Study concept and design: Ashok J. Theruvath, Heike Daldrup-Link

Provision of study materials or patients: Ashok J. Theruvath, Ramya Nyalakonda, Ali Rashidi, Robert Steffner, Rafi Avedian, Sheri Spunt, Heike Daldrup-Link

Imaging: Ashok J. Theruvath, Ali Rashidi, Heike Daldrup-Link

Analysis and interpretation of data: Ashok J. Theruvath, Heike Daldrup-Link

Drafting the manuscript: Ashok J. Theruvath, Ramya Nyalakonda, Heike Daldrup-Link

All authors read and approved the final manuscript.

Conflict of interest

The authors declare that they have no conflict of interest.

Ethics approval

This study was approved by the Stanford Ethics Committee, the Institutional Review board (IRB# 20221). This study was performed in accordance with the principles of Good Clinical Practice and the Declaration of Helsinki and its later amendments or comparable ethical standards.

Consent to participate

All patients or their legal representative gave written informed consent before participating in this study. In addition to parental consent, pediatric patients provided their verbal and written assent to participate.

Results: MRI scans at 24 hours after intravenous ferumoxytol infusion demonstrated a positive T1-enhancement of the effusion in all joints and pleural spaces with tumor infiltration and no joint or pleural space without infiltration. Corresponding SNR (P=0.004) and CNR values (P=0.004) were significantly higher for joints and pleural spaces with than without tumor infiltration. By contrast, unenhanced MRI, Gd-enhanced MRI and 1 hour postcontrast ferumoxytol-MRI did not show any enhancement of the joint or pleural effusion, with or without tumor infiltration.

Conclusion: This pilot study suggests that 24 hour postcontrast ferumoxytol-MRI scans can non-invasively differentiate between joints with and without tumor infiltration.

Keywords

MR Imaging; Iron Oxide Nanoparticles; Molecular Imaging; Pediatric Cancers; Joint; Children; Young Adults

Introduction

The diagnosis of a joint infiltration by a malignant bone tumor is important, because it changes surgical management [1, 2]: Patients with bone tumors that infiltrate a joint require an *en bloc* extra-articular resection of the entire joint with joint capsule and peri-articular muscles, which can be associated with poor functional outcome [2]. Conversely, patients with bone tumors that do not infiltrate the joint are treated with a less extensive intra-articular resection. Preoperative staging of bone sarcomas with magnetic resonance imaging (MRI) has a limited specificity for the diagnosis of a tumor infiltration, ranging from 69% [3] to 73% [4]. False positives lead to unnecessary extensive surgical resections and false negatives can lead to local recurrences and decreased overall survival [3, 5]. Therefore, imaging biomarkers that can improve the specificity of MRI for the detection of tumor joint infiltration are urgently needed.

During our MR imaging evaluations of pediatric and young adult patients with the nanoparticle compound ferumoxytol (Feraheme), we observed a surprising marked T1-enhancement of joint and pleural effusions in some patients and not others. In patients with apparent nanoparticle leak into the joint or pleural effusion, an additional MRI with gadolinium-based contrast agents (GBCA) did not show an enhancement of the joint or pleural effusion. To our knowledge, there is no data on ferumoxytol enhancement of joint or pleural effusions. It has been well described that a malignant effusion by a tumor can lead to an exudate, i.e. a fluid accumulation in the joint, which is associated with an increased microvascular permeability of the synovium and enables extravasation of large molecules such as proteins into the joint compartment [6, 7]. On the other hand, tumors that do not infiltrate the joint can also lead to a reactive fluid accumulation in the joint [3, 8]. Based on our observation, we hypothesized that a malignant tumor infiltration of a joint or pleura would cause an extravasate and nanoparticle leak, while a reactive effusion without tumor joint or pleural infiltration would cause a transudate and no nanoparticle leak. The purpose of this study was to evaluate, if nanoparticle extravasation into joint or pleural effusions differed between joints and pleura with and without tumor infiltration.

Materials and methods:

Patients

This investigation was part of a prospective clinical trial, which investigated the use of ferumoxytol for cancer imaging of pediatric and young adult patients (NCT01542879) and was approved by the institutional review board (IRB) at our institution. Ferumoxytol is an FDA-approved iron supplement, which we used “off label” as an MRI contrast agent through an investigator-initiated investigative new drug application (IND 111,154). We identified 15 pediatric and young adult patients with malignant bone tumors who underwent 18 ferumoxytol-enhanced MRI scans and who met the following inclusion criteria: (1) age less than 30 years, (2) diagnosis of a malignant bone tumor with effusion and (3) MRI scan with intravenously injected ferumoxytol. We included 15 patients with a mean age of 16 years (range: 9–24 years): These included 9 boys (mean age: 15 years, range: 14–18 years) and 6 girls (mean age: 19 years, range: 13–24 years) with osteosarcoma (n=12), Ewing sarcoma (n=2) and undifferentiated sarcoma (n=1) (Table 1). Joint effusion was localized in the hip joint (n=3), knee joint (n=7) or shoulder joint (n=1). Four patients had the tumor in the rib (n=1) or metastasized to the chest (n=3) with infiltration of the pleura and a pleural effusion (Table 1). Ferumoxytol was diluted 1:3 in saline and administered at a dose of 5 mg Fe/kg bodyweight over 15 minutes as recommended by the food and drug administration (FDA) [9]. We monitored the heart rate and blood pressure of the patients for at least one hour before, during and after the ferumoxytol infusion, and until the patient finished the MRI scan. We also asked the patients for any subjective side effects. All patients or their legal representative gave written informed consent before participating in this study. In addition to parental consent, pediatric patients provided their verbal and written assent to participate.

MR Imaging

All patients underwent a ferumoxytol-enhanced MRI at 1 hour (n=7) or 24 hours (n=11) after intravenous injection of ferumoxytol. Three of the patients had two ferumoxytol-enhanced MRI scans, two patients with baseline and post induction chemotherapy scans and one patient with MRI 1 hour and 24 hours after ferumoxytol injection. MRI scans were obtained on a 3T PET/MRI scanner (n=14, Signa GE Healthcare, Milwaukee, USA) or a 3T MRI scanner (n=4, Discovery 750 GE Healthcare, Milwaukee, USA), using the following sequences: T2-weighted fast spin echo (FSE) sequences (TR = 4000 ms, TE = 116 ms, flip angle (α) = 111°, slice thickness (SL) = 3 mm), PD-weighted FSE sequences (TR / TE / α = 4538 / 29 / 111, SL = 3 mm), T1-weighted FSE sequences (TR / TE / α = 709 / 7.8 ms / 111, SL = 3 mm), and LAVA sequences (TR / TE / α = 9.5 / 1.3 / 15, SL = 3.4 mm). For patients who had the lesion in their chest an additional T2 PROPELLER sequence (TR / TE / α = 12500 / 119 / 110, SL = 4 mm) was acquired. Twelve of the 15 patients had also a separate gadobutrol (Gadavist)-enhanced MRI on a 3T MRI scanner with the same sequences as above within three weeks of the ferumoxytol scan (range: −23 days – 10 days ; mean: −7 days; median: −4 days).

Effusion Assessment

Interpretation of MRI results and effusion assessment was performed by one experienced radiologist (HDL) with more than 20 years of experience. One 4th year radiology resident (AJT) and one medical imager (AR) with three years of experience in musculoskeletal radiology independently measured the signal intensity (SI) of the effusion and standard deviation (SD) of the background on LAVA sequences by drawing regions of interest in the joint or pleural effusion, muscle and background (air surrounding the patient) and calculated the signal to noise ratio (SNR) as:

$$SNR = \frac{SI(effusion)}{SD(background)}$$

In addition, we determined the contrast to noise ratio (CNR) between effusions and muscle as an internal standard as:

$$CNR = \frac{(SNR(effusion) - SNR(muscle))}{SNR(muscle)}$$

The readers were blinded to type of contrast agent, timing of the scan, histopathologic findings and clinical information.

Standard of Reference

In all resected tumors (n=11), positive tumor infiltration status was assessed based on histopathological evaluation of joint or pleural invasion with a mean interval between ferumoxytol-enhanced MRI and surgery of 60 days (median: 70 days; range: 6–82 days). Eight of the 11 patients had neoadjuvant chemotherapy between ferumoxytol-enhanced MRI and surgery and three patients had surgery ultimately after ferumoxytol enhanded-MRI (mean: 12 days; median: 7 days; range: 6–24 days). If no histopathology was available (n=4) the previously described MRI-based criteria, such as cortex disruption of an intra-articular bone component or visible intra-articular tumor nodules were applied [10]. Based on these data, we defined two groups of tumors with and without joint or pleural infiltration.

Statistical Analysis

Interobserver agreement was measured by a two-way mixed intra-class correlation coefficient analysis [11]. SNR and CNR values of patients with positive and negative infiltration status were compared on unenhanced LAVA scans (n=13), gadolinium-enhanced LAVA scans (n=13), 1 hour (n=7) and 24 hour ferumoxytol-enhanced LAVA scans (n=11), using a Mann-Whitney test. Due to multiple comparisons of infiltration status with SNR and CNR within the same patients (n=6), we applied the Bonferroni correction and considered P values < 0.008 to be statistically significant. All statistical tests were performed using GraphPad Prism (version 6.0, San Diego, CA, USA) and SPSS (version 28, IBM, Armonk, NY).

Results:

Interobserver agreement was excellent for measurements of SNR and CNR of joint or pleural effusions for unenhanced, gadolinium-enhanced and ferumoxytol-enhanced MRI scans at 1 hour and 24 hours (Table 2). Unenhanced T1-weighted LAVA scans demonstrated a hypointense signal of the joint or pleural effusion in all patients. T1-weighted LAVA scans at 24 hours after ferumoxytol infusion (n=11) demonstrated a positive (bright) T1-enhancement of the effusion in patients with tumor joint infiltration (Fig. 1, 2) and a positive (bright) T1-enhancement of a pleural effusion in patients with infiltrative tumors of the chest wall (Fig. 3). By comparison, patients without tumor joint or pleural infiltration demonstrated no or minimal T1-enhancement of the effusion, when compared to muscle as a reference tissue (Fig. 4). Corresponding SNR values were significantly higher for effusions with tumor infiltration compared to effusions without tumor infiltration (1739±159 vs 99±12; P=0.004). Similarly, CNR values of effusions were also significantly higher in tumors with infiltration compared to tumors without infiltration (1.19±0.13 vs. −0.33±0.07; P=0.004).

By contrast, unenhanced T1-weighted scans (n=13), Gd-enhanced scans (n=13) and ferumoxytol-enhanced scans at 1 hour after ferumoxytol infusion (n=7) did not show any enhancement of the effusions in the presence or absence of joint or pleural infiltration (Fig. 4). SNR and CNR values were not significantly different between patients with positive and negative infiltration status on unenhanced LAVA (SNR: 47.71±9.17 vs. 52.15±11.79; P=0.71 and CNR: −0.36±0.12 vs. −0.36±0.11; P=0.81), gadolinium-enhanced LAVA (SNR: 31.14±7.72 vs. 47.28±10.79; P=0.29 and CNR: −0.43±0.11 vs. −0.49±0.10; P=0.87) and 1 hour ferumoxytol-enhanced LAVA scans (SNR: 87.22±7.58 vs. 102.30±24.65; P=0.86 and CNR: −0.15±0.06 vs. −0.12±0.02; P= 0.99).

Discussion:

Our pilot study suggests that ferumoxytol leakage into a joint or pleural effusion might be a surrogate marker for joint or plerual infiltration of bone sarcomas. Ferumoxytol-enhanced MRI scans at 24 hours after nanoparticle injection (n=11) demonstrated a strong T1-enhancement of joint and pleural effusions in patients with tumor infiltration (n=6), while there was no significant T1-enhancement of joint or pleural effusions in patients without tumor infiltration (n=5). To our knowledge, this is the first study, which shows leakage of intravenously injected ferumoxytol into the joint or pleural effusion of tumor infiltrated joints or pleural spaces.

Small molecular gadolinium chelates rapidly distribute from the blood to the interstitium of normal visceral organs and various pathologies, including both benign and malignant tumors and are excreted with a plasma half-life of 70–90 minutes [12, 13]. By comparison, ferumoxytol nanoparticles are significantly larger (30 nm), have a longer plasma half-life of 14 to 21 hours and do not extravasate into most normal organs [9]. In tumors, several investigators [14] including our own group [15] reported a differential microvascular permeability of iron oxide nanoparticles in benign and malignant tumors: Iron oxide nanoparticles extravasated across the leaky microvessels in malignant tumors, but not

across the intact microvessel wall of benign tumors. This led to a positive enhancement of malignant tumor, but not benign tumors [15].

Similarly, our studies here demonstrates leakage of ferumoxytol nanoparticles into joint or pleural effusions that were infiltrated with tumors while no ferumoxytol leakage was noted into joint or pleural effusions that were not infiltrated with tumors. This differential enhancement of malignant and reactive effusions can be explained by the biological concept of exudates and transudates: An exudate is due to an increased endothelial permeability and leads to extravasation of macromolecules such as proteins from the blood [6]. We postulate that the same mechanism leads to an extravasation of ferumoxytol nanoparticles. Conversely, a transudate is due to an imbalance in hydrostatic and oncotic pressures and does not lead to extravasation of macromolecules [16, 17]. Accordingly, we did not find an extravasation of ferumoxytol nanoparticles into joints or pleural effusions with transudates.

Our data also shows that the extravasation of ferumoxytol nanoparticles into effusions takes time: We observed a marked ferumoxytol leakage into malignant effusions on MRI scans at 24 hours after intravenous ferumoxytol administration, but not at 1 hour. This is consistent with previous observations in malignant tumors, which showed that the accumulation of ferumoxytol in glioblastomas [18], lymphomas [18] and sarcomas [19] slowly increased over 24 hours, both in animal models [19] and in patients [18]: A strong tumor T1 signal enhancement was noted at 24 hours after ferumoxytol infusion, but not at 1 hour postcontrast [19]. We recently described that ferumoxytol can replace gadolinium chelates for evaluation of bone tumors [20]. Therefore, a practical clinical protocol would consist of an intravenous ferumoxytol infusion on day 1 with the addition of a staging chest CT scan and a dedicated 24 hour postcontrast MRI scan of the tumor on day 2.

An extravasation of iron oxide nanoparticles into the synovium and joint effusions is not specific for malignancy, but can be also observed in case of joint infection or inflammation: Simon et al [21] and Lefevre et al [22] reported an extravasation of iron oxide nanoparticles associated with antigen-induced arthritis and septic arthritis in rodent models, which led to marked T1-enhancement of the synovium and the joint fluid. By contrast, normal joints did not show any signs of nanoparticle leak into the joint space. In addition, pathologic fractures could potentially also lead to extravasation of iron oxide nanoparticles into joints or pleural spaces.

We did not notice significant leakage of the small molecular Gd-chelate Gadobutrol into benign or malignant joint or pleural effusions in the early postcontrast phase. This is consistent with previous MR imaging studies in rodents with antigen-induced arthritis [23]. We did not obtain delayed MRI scans after intravenous administration of Gd-chelates. Previous investigators did note an extravasation of Gd-chelates into joint effusions on delayed postcontrast T1-weighted MR images, several hours after intravenous contrast administration. This effect was utilized for indirect arthrographies [24–26]. However, small molecular Gd-chelates leaked into joints of both healthy patients and patients with pathological effusions [27, 28]. This is because small molecules already leak across intact microvessels [27], therefore not allowing for further discrimination between transudates and exudates.

This pilot study was limited by a small sample size. However, cancer in children and young adults is rare and tumor joint infiltration occurs in only 16–22% of patients with bone sarcomas [3, 4, 29, 30]. Patients with bone sarcomas typically undergo neoadjuvant chemotherapy before surgical tumor resection, leading to better local control. Most of our patients also received neoadjuvant chemotherapy prior to surgery. But only three of our patients had a ferumoxytol-enhanced MRI scan directly before surgery with histopathological correlations. Therefore, we cannot exclude false negatives for studies that had neoadjuvant chemotherapy before surgery and histopathology. Likely, the presence or absence of a tumor joint or pleural enhancement will not be binary, but rather a continuum with some intermediate and indeterminate states.

Conclusion:

In summary, our pilot study of bone sarcomas suggests that positive enhancement of joint or pleural fluid on delayed ferumoxytol-enhanced MRI indicates tumor infiltration. Thus, ferumoxytol-induced joint enhancement on 24 hour postcontrast scans can impact surgical management of these patients. A positive T1-signal enhancement of a joint effusion in a patient with bone sarcoma could increase the confidence towards planning of a more invasive surgery with en-bloc resection of the entire joint. Conversely, patients without nanoparticle joint enhancement could be directed to less invasive surgical procedures with lower complication rates and better functional outcomes. Ultimately, our imaging test could improve the quality of life and help preserve limb function of pediatric and young adult cancer patients.

Acknowledgements:

This work was in part supported by a grant from the Eunice Kennedy Shriver National Institute of Child Health and Human Development, grant number R01 HD081123-01A1 and the Sarcoma Foundation of America. We thank Mehdi Khalighi, Dawn Holley and Kim Halbert from the PET/MR Metabolic Service Center for their assistance with the acquisition of PET/MR scans at the Lucas Research Center at Stanford.

Availability of data and material

All data and material support our published claims and comply with the field standards and are available from the corresponding author upon reasonable request.

References:

1. Sim IW, Tse LF, Ek ET, Powell GJ, Choong PF (2007) Salvaging the limb salvage: management of complications following endoprosthetic reconstruction for tumours around the knee. Eur J Surg Oncol 33:796–802. doi: 10.1016/j.ejso.2006.10.007 [PubMed: 17291709]
2. Shahid M, Albergo N, Purvis T, Heron K, Gaston L, Carter S, Grimer R, Jeys L (2017) Management of sarcomas possibly involving the knee joint when to perform extra-articular resection of the knee joint and is it safe? Eur J Surg Oncol 43:175–180. doi: 10.1016/j.ejso.2016.05.018 [PubMed: 27266818]
3. Schima W, Amann G, Stiglbauer R, Windhager R, Kramer J, Nicolakis M, Farres MT, Imhof H (1994) Preoperative staging of osteosarcoma: efficacy of MR imaging in detecting joint involvement. AJR Am J Roentgenol 163:1171–1175. doi: 10.2214/ajr.163.5.7976895 [PubMed: 7976895]

4. Ozaki T, Putzke M, Burger H, Gosheger G, Winkelmann W, Lindner N (2002) Infiltration of sarcomas into the hip joint: comparison of CT, MRI and histologic findings in 67 cases. Acta Orthop Scand 73:220–226. doi: 10.1080/000164702753671849 [PubMed: 12079023]
5. Zuckerman SL, Amini B, Lee SH, Rao G, Tatsui CE, Rhines LD (2019) Predictive Value of Preoperative Magnetic Resonance Imaging Findings for Survival and Local Recurrence in Patients Undergoing En Bloc Resection of Sacral Chordomas. Neurosurgery 85:834–842. doi: 10.1093/neuros/nyy578 [PubMed: 30541143]
6. Tamsma JT, Keizer HJ, Meinders AE (2001) Pathogenesis of malignant ascites: Starling's law of capillary hemodynamics revisited. Ann Oncol 12:1353–1357. doi: 10.1023/a:1012504904713 [PubMed: 11762804]
7. Stein-Werblowsky R (1980) A permeability-enhancing factor produced by tumor. The genesis of malignant effusions. J Cancer Res Clin Oncol 97:315–320. doi: 10.1007/BF00405784 [PubMed: 6160159]
8. Quan GM, Slavin JL, Schlicht SM, Smith PJ, Powell GJ, Choong PF (2005) Osteosarcoma near joints: assessment and implications. J Surg Oncol 91:159–166. doi: 10.1002/jso.20268 [PubMed: 16118770]
9. Toth GB, Varallyay CG, Horvath A, Bashir MR, Choyke PL, Daldrup-Link HE, Dosa E, Finn JP, Gahramanov S, Harisinghani M, Macdougall I, Neuwelt A, Vasanawala SS, Ambady P, Barajas R, Cetas JS, Ciporen J, DeLoughery TJ, Doolittle ND, Fu R, Grinstead J, Guimaraes AR, Hamilton BE, Li X, McConnell HL, Muldoon LL, Nesbit G, Netto JP, Petterson D, Rooney WD, Schwartz D, Szidonya L, Neuwelt EA (2017) Current and potential imaging applications of ferumoxytol for magnetic resonance imaging. Kidney international 92:47–66. doi: 10.1016/j.kint.2016.12.037 [PubMed: 28434822]
10. Holzapfel K, Regler J, Baum T, Rechl H, Specht K, Haller B, von Eisenhart-Rothe R, Gradinger R, Rummeny EJ, Woertler K (2015) Local Staging of Soft-Tissue Sarcoma: Emphasis on Assessment of Neurovascular Encasement-Value of MR Imaging in 174 Confirmed Cases. Radiology 275:501–509. doi: 10.1148/radiol.14140510 [PubMed: 25584707]
11. Zidan M, Thomas RL, Slovis TL (2015) What you need to know about statistics, part II: reliability of diagnostic and screening tests. Pediatric radiology 45:317–328. doi: 10.1007/s00247-014-2944-x [PubMed: 25726014]
12. Runge VM (2017) Critical Questions Regarding Gadolinium Deposition in the Brain and Body After Injections of the Gadolinium-Based Contrast Agents, Safety, and Clinical Recommendations in Consideration of the EMA's Pharmacovigilance and Risk Assessment Committee Recommendation for Suspension of the Marketing Authorizations for 4 Linear Agents. Invest Radiol 52:317–323. doi: 10.1097/rli.0000000000000374 [PubMed: 28368880]
13. Aime S, Caravan P (2009) Biodistribution of gadolinium-based contrast agents, including gadolinium deposition. Journal of magnetic resonance imaging : JMRI 30:1259–1267. doi: 10.1002/jmri.21969 [PubMed: 19938038]
14. Harisinghani MG, Saini S, Weissleder R, Hahn PF, Yantiss RK, Tempany C, Wood BJ, Mueller PR (1999) MR lymphangiography using ultrasmall superparamagnetic iron oxide in patients with primary abdominal and pelvic malignancies: radiographic-pathologic correlation. AJR Am J Roentgenol 172:1347–1351. doi: 10.2214/ajr.172.5.10227514 [PubMed: 10227514]
15. Daldrup-Link HE, Rydland J, Helbich TH, Bjornerud A, Turetschek K, Kvistad KA, Kaindl E, Link TM, Staudacher K, Shames D, Brasch RC, Haraldseth O, Rummeny EJ (2003) Quantification of breast tumor microvascular permeability with feruglose-enhanced MR imaging: initial phase II multicenter trial. Radiology 229:885–892. doi: 10.1148/radiol.2293021045 [PubMed: 14576446]
16. Kinasewitz GT (1997) Transudative effusions. Eur Respir J 10:714–718. [PubMed: 9073011]
17. D'Agostino HP, Edens MA (2020) Physiology, Pleural Fluid. StatPearls, Treasure Island (FL).
18. Bashir MR, Bhatti L, Marin D, Nelson RC (2015) Emerging applications for ferumoxytol as a contrast agent in MRI. Journal of magnetic resonance imaging : JMRI 41:884–898. doi: 10.1002/jmri.24691 [PubMed: 24974785]
19. Aghighi M, Golovko D, Ansari C, Marina NM, Pisani L, Kurlander L, Klenk C, Bhaumik S, Wendland M, Daldrup-Link HE (2015) Imaging Tumor Necrosis with Ferumoxytol. PloS one 10:e0142665. doi: 10.1371/journal.pone.0142665 [PubMed: 26569397]

20. Siedek F, Muehe AM, Theruvath AJ, Avedian R, Pribnow A, Spunt SL, Liang T, Farrell C, Daldrup-Link HE (2020) Comparison of ferumoxytol- and gadolinium chelate-enhanced MRI for assessment of sarcomas in children and adolescents. Eur Radiol 30:1790–1803. doi: 10.1007/s00330-019-06569-y [PubMed: 31844962]
21. Simon GH, von Vopelius-Feldt J, Fu Y, Schlegel J, Pinotek G, Wendland MF, Chen MH, Daldrup-Link HE (2006) Ultrasmall supraparamagnetic iron oxide-enhanced magnetic resonance imaging of antigen-induced arthritis: a comparative study between SHU 555 C, ferumoxtran-10, and ferumoxytol. Invest Radiol 41:45–51. [PubMed: 16355039]
22. Lefevre S, Ruimy D, Jehl F, Neuville A, Robert P, Sordet C, Ehlinger M, Dietemann JL, Bierry G (2011) Septic arthritis: monitoring with USPIO-enhanced macrophage MR imaging. Radiology 258:722–728. doi: 10.1148/radiol.10101272 [PubMed: 21339348]
23. Simon GH, von Vopelius-Feldt J, Wendland MF, Fu Y, Piontek G, Schlegel J, Chen MH, Daldrup-Link HE (2006) MRI of arthritis: comparison of ultrasmall superparamagnetic iron oxide vs. Gd-DTPA. Journal of magnetic resonance imaging : JMRI 23:720–727. doi: 10.1002/jmri.20556 [PubMed: 16557494]
24. Osinski T, Malfair D, Steinbach L (2006) Magnetic resonance arthrography. The Orthopedic clinics of North America 37:299–319, vi. doi: 10.1016/j.ocl.2006.04.002 [PubMed: 16846763]
25. Morrison WB (2005) Indirect MR arthrography: concepts and controversies. Semin Musculoskelet Radiol 9:125–134. doi: 10.1055/s-2005-872338 [PubMed: 16044381]
26. Jaramillo D, Laor T (2008) Pediatric musculoskeletal MRI: basic principles to optimize success. Pediatric radiology 38:379–391. doi: 10.1007/s00247-007-0645-4 [PubMed: 18046547]
27. Winalski CS, Aliabadi P, Wright RJ, Shortkroff S, Sledge CB, Weissman BN (1993) Enhancement of joint fluid with intravenously administered gadopentetate dimeglumine: technique, rationale, and implications. Radiology 187:179–185. doi: 10.1148/radiology.187.1.8451409 [PubMed: 8451409]
28. Yamato M, Tamai K, Yamaguchi T, Ohno W (1993) MRI of the knee in rheumatoid arthritis: Gd-DTPA perfusion dynamics. J Comput Assist Tomogr 17:781–785. doi: 10.1097/00004728-199309000-00022 [PubMed: 8370835]
29. Simon MA, Hecht JD (1982) Invasion of joints by primary bone sarcomas in adults. Cancer 50:1649–1655. doi: 10.1002/1097-0142(19821015)50:8<1649::aid-cncr2820500832>3.0.co;2-g [PubMed: 6956428]
30. Brisse H, Ollivier L, Edeline V, Pacquement H, Michon J, Glorion C, Neuenschwander S (2004) Imaging of malignant tumours of the long bones in children: monitoring response to neoadjuvant chemotherapy and preoperative assessment. Pediatric radiology 34:595–605. doi: 10.1007/s00247-004-1192-x [PubMed: 15103428]

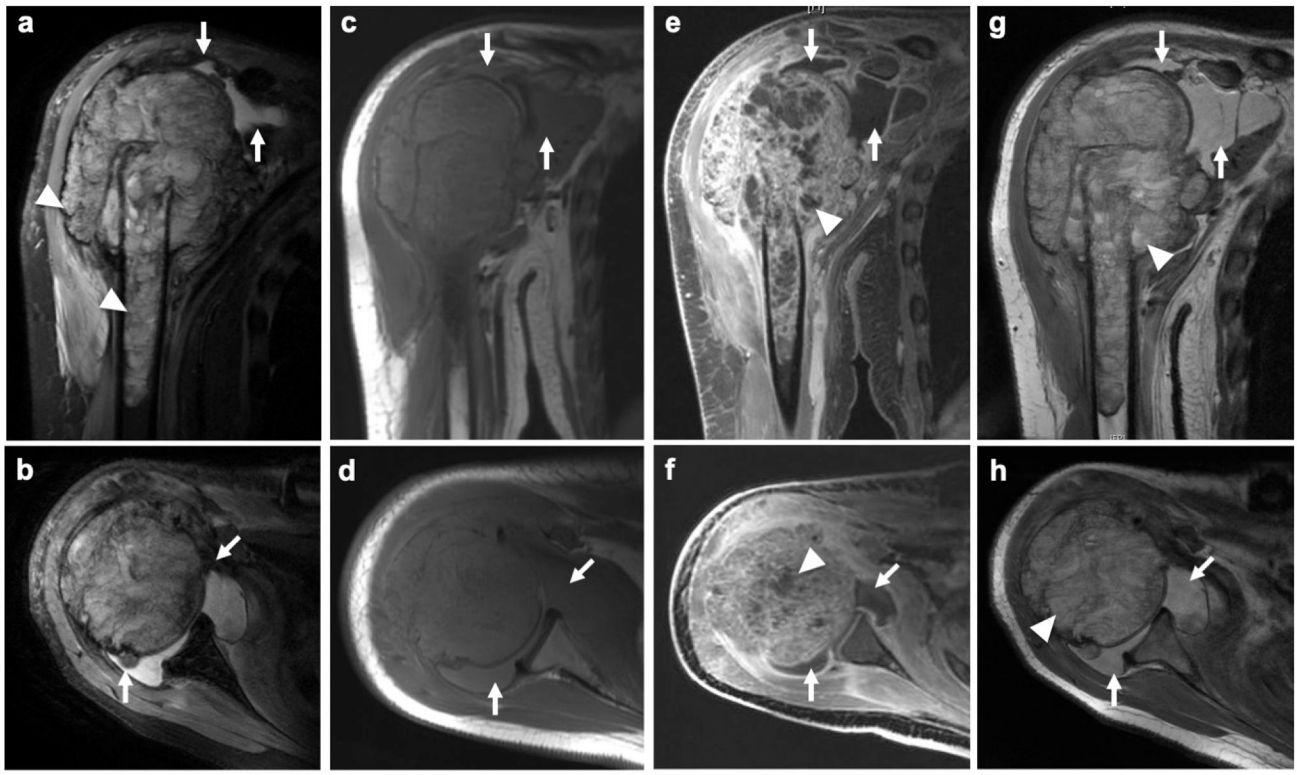

Fig.1.

Ferumoxytol leak into a joint effusion of a 13-year old female patient with an osteosarcoma of the proximal right humerus. **a** Coronal PD-weighted fast spin echo (FSE) image demonstrates an inhomogenous intra- and extra-osseous tumor of the proximal humerus (arrowheads) with joint effusion (arrows). **b** Corresponding axial PD-weighted FSE image shows tumor joint infiltration (arrows). **c** Coronal and **d** axial pre-contrast T1-weighted FSE show a hypo- to isointense joint effusion (arrows). **e** Coronal and **f** axial LAVA images after intravenous injection of gadobutrol demonstrates inhomogenous enhancement of the tumor (arrowheads) and the synovia. The effusion (arrows) does not enhance. **g** Coronal and **g** axial T1-weighted FSE image at 24 hours after ferumoxytol administration demonstrates T1-enhancement of the tumor (arrowheads) and the joint effusion (arrows)

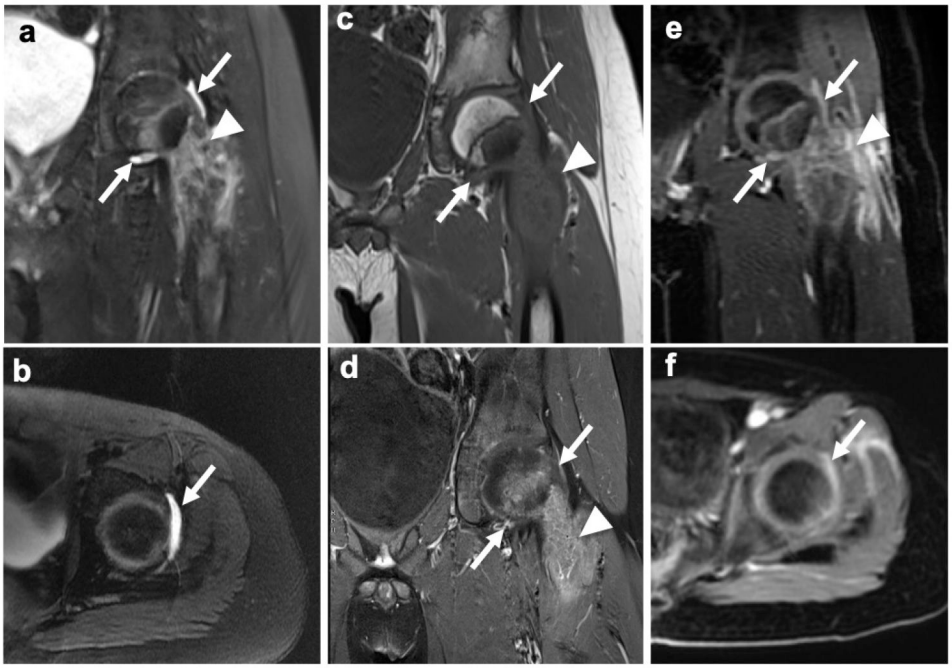

Fig. 2.

Subtle ferumoxytol leak into a joint effusion of 9-year old male patient with an osteosarcoma in the proximal left femur and unclear infiltration status based on unenhanced and gadolinium-enhanced MR imaging. **a,b** Coronal and axial T2-weighted fast spin echo (FSE) images show an inhomogeneous tumor in the proximal left femur (arrowhead) and a subtle joint effusion (arrows). **c** Corresponding pre-contrast coronal T1-weighted FSE image and **d** post-gadolinium T1-weighted FSE image with fat saturation show no definite signs of joint infiltration and no enhancement of the effusion (arrows). **e,f** However, on coronal and axial ferumoxytol-enhanced LAVA images at 24 hours a hyperintense signal of the joint effusion is demonstrated, suggesting ferumoxytol leakage.

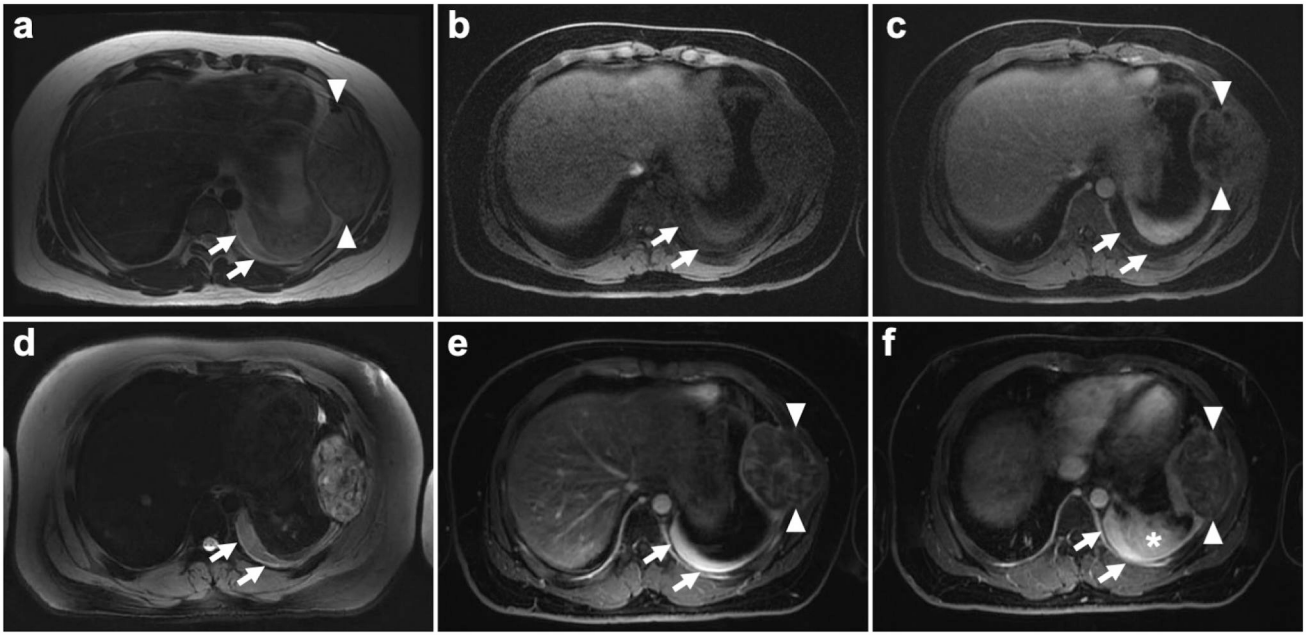

Fig. 3.

Enhancement of pleural effusion 24 hours after ferumoxytol administration in a 16-year old male patient with Ewing sarcoma of the left 7th rib. **a** Axial T2 scan shows hyperintense pleural effusion (arrows) in the dorsal part of the left lung and a Ewing sarcoma in the left 7th rib (arrowheads). **b,c** Pre and post gadolinium LAVA images show hypointense pleural effusion (arrows) and inhomogenous gadolinium uptake of the Ewing sarcoma (arrowheads). **d** On the following day, 24 hours after intravenous ferumoxytol injection axial T2 PROPELLER images show a stable hyperintense pleural effusion (arrows). **e,f** However, on LAVA sequences the pleural effusion showed marked ferumoxytol enhancement (arrows), suggesting leakage of iron oxide nanoparticles from the Ewing sarcoma (arrowheads) in the left 7th rib. Of note also potential leakage from adjacent opacity in the left dorsal lung (asterisk)

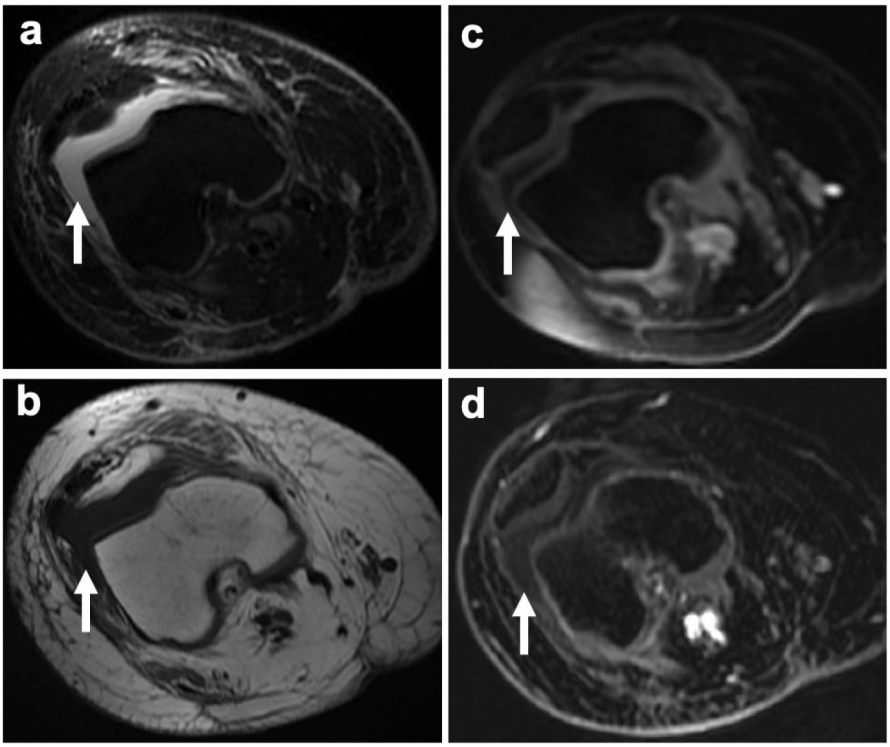

Fig. 4.

Knee joint effusion without T1-enhancement in a 24-year old female patient with recurrence of osteosarcoma in the right femur. **a** Axial PD-weighted FSE image shows a hyperintense knee joint effusion (arrow). **b** Corresponding pre-contrast axial T1-weighted FSE images demonstrates a hypointense joint effusion (arrow)**. c** Post gadolinium and **d** 1 hour post ferumoxytol LAVA images show a hypointense knee joint effusion without T1-enhancement (arrows)

Table 1

Patient Characteristics

Patient	Diagnosis	Effusion Site	Baseline Ferumoxytol MRI (Y/N)		Post-Neoadjuvant Ferumoxytol MRI (Y/N)		Reference Standard (MRI/ Pathology)
			1 hour	24 hour	1 hour	24 hour	
1	Ewing sarcoma	Left Hip	Y	N	N	N	MRI
2	Osteosarcoma	Right Knee	Y	Y	N	N	Pathology
3	Osteosarcoma	Right Knee	N	Y	N	N	Pathology
4	Osteosarcoma	Pleura	N	Y	N	N	MRI
5	Osteosarcoma	Right Knee	N	Y	N	Y	Pathology
6	Osteosarcoma	Right Knee	N	N	Y	N	MRI
7	Osteosarcoma	Right Shoulder	N	Y	N	Y	Pathology
8	Osteosarcoma	Right Hip	Y	N	N	N	Pathology
9	Undifferentiated sarcoma	Pleura	Y	N	N	N	Pathology
10	Osteosarcoma	Right Knee	Y	N	N	N	MRI
11	Ewing sarcoma	Pleura	N	Y	N	N	Pathology
12	Osteosarcoma	Right Knee	N	Y	N	N	Pathology
13	Osteosarcoma	Left Hip	N	Y	N	N	Pathology
14	Osteosarcoma	Right Knee	Y	N	N	N	Pathology
15	Osteosarcoma	Pleura	N	Y	N	N	Pathology

Table 2

Interobserver agreement for SNR and CNR measurements of two readers

		Interobserver agreement
SNR	Unenhanced	0.974 (95% CI 0.915–0.992)
	Gd	0.945 (95% CI 0.819–0.983)
	Fe 1h	0.983 95% CI (0.902–0.997)
	Fe 24h	0.997 (95% CI 0.988–0.999)
CNR	Unenhanced	0.951 (95% CI 0.838–0.985)
	Gd	0.965 (95% CI 0.887–0.989)
	Fe 1h	0.914 (95% CI 0.499–0.985)
	Fe 24h	0.995 (95% CI 0.983–0.999)

SNR signal to noise ratio, *CNR* contrast to noise ratio, *CI* confidence interval, *Gd* gadolinium-enhanaced MRI, *Fe* ferumoxytol-enhanced MRI